PHASE MANIPULATION AND THE HARMONIC COMPONENTS OF RINGING FORCES ON A SURFACE-PIERCING COLUMN

C. Fitzgerald[1], J. Grice[1] P.H. Taylor[1], R. Eatock Taylor[1], J. Zang[2]

[1]Department of Engineering Science, University of Oxford
[2]Department of Architecture and Civil Engineering, University of Bath

colm.fitzgerald@eng.ox.ac.uk (presenting author) james.grice@eng.ox.ac.uk
paul.taylor@eng.ox.ac.uk r.eatocktaylor@eng.ox.ac.uk j.zang@bath.ac.uk

The Stokes-type expansion for the hydrodynamic force on a column in a regular wave can be written to 4th order as

$$F = f_{11} a \cos\phi + f_{22} a^2 \cos 2\phi + f_{33} a^3 \cos 3\phi + f_{44} a^4 \cos 4\phi + f_{20} a^2 + f_{31} a^3 \cos\phi + f_{42} a^4 \cos 2\phi$$

where the coefficients f represent wave to force transfer functions (including implicit phase shifts) and a is the incoming linear wave amplitude. Note the structure of the terms multiplying coefficients such as f_{33} where the power of the amplitude term is the same as the frequency harmonic (here both 3), and the terms multiplying terms such as f_{42} where the power of the amplitude is greater than that of the frequency harmonic by 2. In the notation of Stokes expansions, these correspond to sum and difference components respectively. For ringing we are mostly concerned with the sum harmonics. Whilst these individual harmonic components are easy to extract for regular wave forcing, this is much more difficult for broadbanded waves trains, either random or wave groups, where the simple Stokes terms are replaced by summations of products of linear terms and each net higher harmonic contributes across an increasingly broad range of frequencies. There are then strict limits as to what can be achieved by simple frequency filtering.

Here we are concerned with the nonlinear force components generated by isolated compact wave groups impacting on a single surface piercing column. The experiments were performed in the shallow water wave basin at DHI and reported at a previous workshop [1] and at Coastlab 2010 [2]. The cylinder diameter was 0.25*m* and the water depth 0.505*m*. The total horizontal hydrodynamic load was inferred from the horizontal force transmitted through strain gauges to a stiff supporting frame, after accounting for the structural dynamics of the mechanical system (resonant freq 3.88*Hz*, 0.9% of critical damping).

We report results from a series of experiments with a NewWave-type compact uni-directional wave group with a spectral peak frequency of 0.61*Hz*, and an amplitude at focus of ~ 5*cm*. The overall aim is to compare measured load components to linear and 2nd order diffraction theory, using the code DIFFRACT (eg. Zang et al. [3]). We also use a fully nonlinear boundary element potential flow solver (OXPOT, based on Bai & Eatock Taylor [4], which uses quadratic free surface triangles) to extract the harmonic structure with an apparently novel phase-based separation method. For this we use 4 runs of OXPOT, each with the same input paddle signal, except that the phase of each Fourier component is shifted by 0, 90, 180 (inverted) and 270°, leading to the resulting force time histories *F*0, *F*1, *F*2 and *F*3. We then seek to extract the individual Stokes-type components by linear combinations of these signals, including their Hilbert transforms (denoted by h), rather than depending on frequency separation of the signals. Up to the 4th harmonic, simple linear combinations of the 4 phase-shifted runs yield

$$[F0 - F1h - F2 + F3h]/4 = f_{11} a\cos\phi + f_{31} a^3 \cos\phi$$
$$[F0 - F1 + F2 - F3]/4 = f_{22} a^2 \cos 2\phi + f_{42} a^4 \cos 2\phi$$
$$[F0 + F1h - F2 - F3h]/4 = f_{33} a^3 \cos 3\phi$$
$$[F0 + F1 + F2 + F3]/4 = f_{20} a^2 + f_{44} a^4 \cos 4\phi$$

Only for the 4th harmonic is there an overlap with the 2nd order difference long wave loading, and these are simple to separate by frequency filtering. Thus, running 4 phase shifted cases yields the dominant harmonic components up to the 4th sum harmonic. We note in passing the relative importance of the difference terms, such as f_{31} compared to the f_{11} term. These terms have the same frequency content but different dependency on the wave amplitude. In general, all such difference terms are likely to be negligible for weakly nonlinear waves, except for the 2nd order difference long-wave f_{20} term.

Only the target wave groups and their inverted forms (0 and 180°) were used in the experiments, so for this data more of the harmonic separation has to be done by frequency filtering. Two combinations yield odd and even harmonics

$$[F0 - F2]/2 = f_{11} a\cos\phi + f_{31} a^3 \cos\phi + f_{33} a^3 \cos 3\phi$$
$$[F0 + F2]/2 = f_{20} a^2 + f_{22} a^2 \cos 2\phi + f_{42} a^4 \cos 2\phi + f_{44} a^4 \cos 4\phi$$

The simple combination for a wave group and the similar but inverted group allows some separation, but not as effectively as the combination of 4 groups with phase shifts of multiples of 90°. We now apply these ideas to the force data obtained for the cylinder at DHI.

The surface elevation time history on the centre-line of the cylinder but in the absence of the cylinder and the total hydrodynamic load are shown in Figure 1. As expected for a weakly nonlinear wave group, the loading is dominated by a linear inertia load component, so the force leads the free-surface elevation by close to 90°. The composite Figure 2 shows the linear frequency component, the 2nd harmonic double and difference frequency terms, the net 3rd and 4th sum harmonics, all as derived from both the physical experiments and the fully nonlinear potential flow simulations. The linear component has also been compared to a Morison inertia prediction using C_m=2 and a linear diffraction result (using DIFFRACT). The cylinder is compact on a wavelength scale so the good agreement between all the linear predictions and the experimental data is to be expected, but still worthy of note as it provides an independent check on the quality of the experiments.

Given the good match for the linear load component, the theoretical 2nd and 4th harmonics also match the measured components well. Even the 2nd harmonic error wave driven by the paddle (because only linear paddle driver signals were used) is clearly represented, centered at ~ 6*s*. We conclude that, for all the components other than the 3rd, the nonlinear potential flow solver is adequate. In contrast, the measured and predicted 3rd harmonic components are rather different. This is interesting as much work has been done on 3rd order forcing, starting with the FNV model from Faltinsen, Vinje and Newman, see [5,6]. Close examination of the 3rd harmonic experimental record shows two significant dips in the envelope of the experimental signal at times ~ 0*s* and 1*s*. This is consistent with two superposed broadbanded components coming in and out of phase. This may be the explanation if, as well as the nonlinear potential flow components, there is also a small drag term. The Morison drag term in a sinusoidal flowfield can be expanded into harmonic components as

$$u|u| \sim a\cos\phi|a\cos\phi| \sim \frac{8}{3\pi}a^2\left(\cos\phi + 1/5\cos 3\phi + \right)$$

so we can immediately identify a 3rd harmonic contribution in frequency (but 2nd order in wave amplitude) arising from the Morison drag term. We speculate that the presence of this drag component in the physical experiment results in the mis-match and, somewhat unusually, it is relatively more significant for small amplitude waves for the 3rd harmonic (in contrast the drag term in the linear frequency range will be small compared to the linear diffraction force component for small waves). Further examples of the harmonic structure of the hydrodynamic loading on a surface-piercing column will be presented at the workshop as well as results from OpenFOAM VOF-type simulations.

In conclusion

- The harmonic structure of the horizontal force on a cylinder excited by compact wave groups with broad spectral content can be extracted using phase shifted combinations, even when simple frequency filtering is unable to achieve satisfactory separation.
- A fully nonlinear potential flow solver appears to capture most of the harmonic structure of the unsteady loading on a surface piercing column except for the 3rd harmonic in frequency.
- The discrepancy between the measured and predicted 3rd harmonic components may be due to a small contribution from a Morison-type drag.

C. Fitzgerald acknowledges the support of the Energy Technologies Institute (ETI) through the PerAWaT project to the University of Oxford for part of this work. The authors want to thank Jens Kirkegaard and all the staff at DHI for their help with the experiments and support through the EU-funded Hydralab III programme.

References:

[1] Zang J., Taylor P.H., Morgan G., Tello M. and Orszaghova J. (2010) Steep wave and breaking wave impact on offshore turbine foundations – ringing re-visited. Proc. 25th IWWWFB, Harbin.

[2] Zang J., Taylor P.H., Morgan G., Tello M. and Orszaghova J. (2010) Experimental study of non-linear wave impact on offshore wind turbine foundations. Proc. 3rd Int. Conf. on the Application of Physical Modelling to Port and Coastal Protection, Coastlab.

[3] Zang J., Gibson R., Taylor P.H. and Eatock Taylor R. (2006) Second order wave diffraction around a fixed ship-shaped body in uni-directional waves. Trans. ASME, JOMAE, 128, 89-99.

[4] Bai W and Eatock Taylor (2006) Fully nonlinear simulation of wave interaction with fixed and floating flared structures. Ocean Eng., 36, 223-236.

[5] Faltinsen O.M., Newman J.N. and Vinje T.E. (1995) Nonlinear wave loads on a slender vertical cylinder. JFM, 289, 179-198.

[6] Newman J.N. (1996) in 'Waves and Nonlinear Processes in Hydrodynamics', ed. Grue J., Kluwer Academic Press, 91-102.

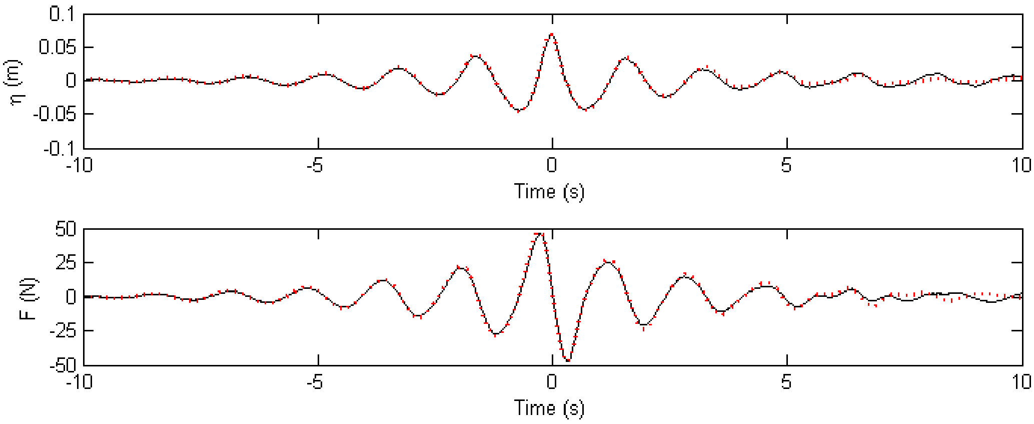

Figure 1. Surface elevation time series (*m*) and applied horizontal force (*N*), experimental data in solid black and fully nonlinear potential flow simulations (OXPOT) in dotted red.

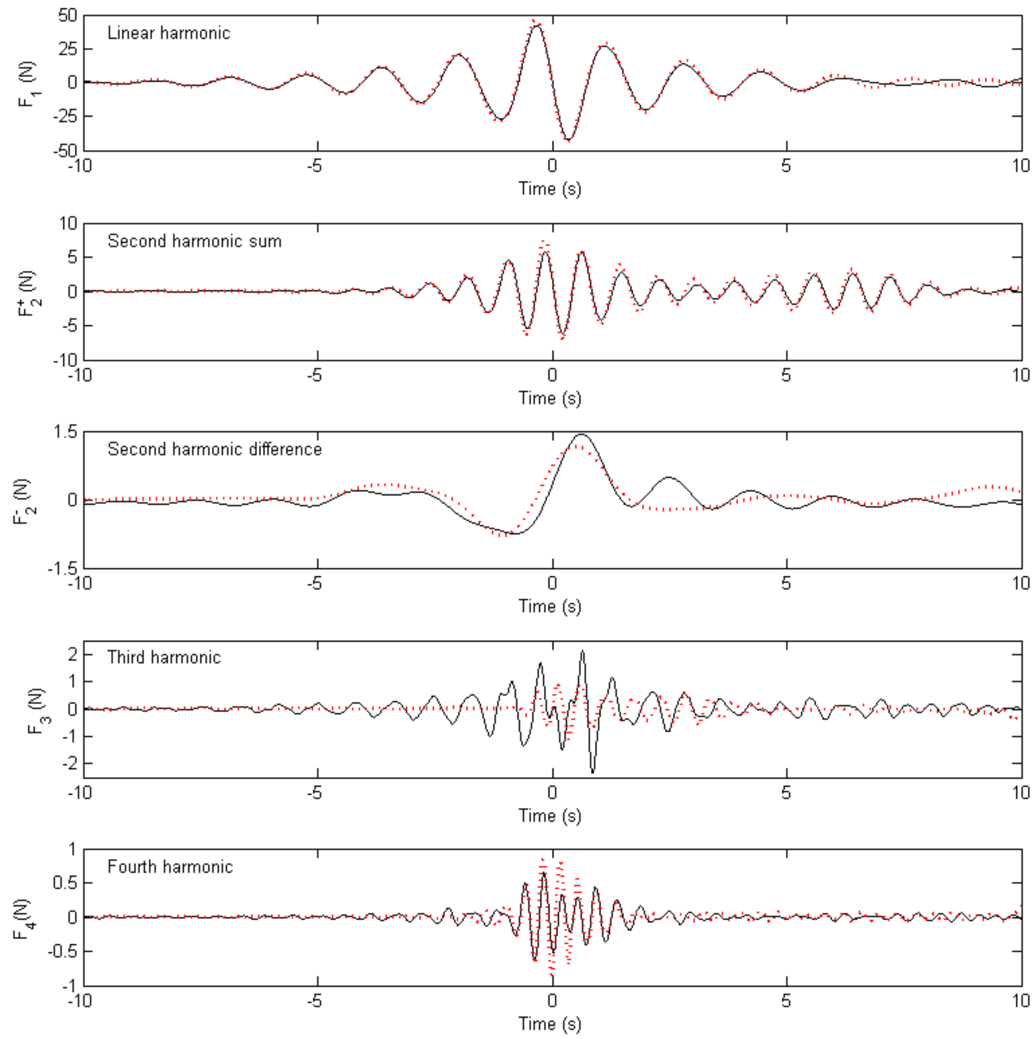

Figure 2. Harmonic decomposition of horizontal force time series, experimental data in solid black and fully nonlinear potential flow simulations (OXPOT) in dotted red.